

Scaling of Anisotropic Flows in Intermediate Energy and Ultra-relativistic Heavy Ion Collisions

Y. G. Ma

Shanghai Institute of Applied Physics, Chinese Academy of Sciences, Shanghai 201800, China

Abstract. Anisotropic flows (v_2 and v_4) of hadrons and light nuclear clusters are studied by a partonic transport model and nucleonic transport model, respectively, in ultra-relativistic and intermediate energy heavy ion collisions. Both number-of-constituent-quark scaling of hadrons, especially for ϕ meson which is composed of strange quarks, and number-of-nucleon scaling of light nuclear clusters are discussed and explored for the elliptic flow (v_2). The ratios of v_4/v_2^2 of hadrons and nuclear clusters are, respectively, calculated and they show different constant values which are independent of transverse momentum. The above phenomena can be understood, respectively, by the coalescence mechanism in quark-level or nucleon-level.

INTRODUCTION

Anisotropic flow is of interesting subject in theoretical and experimental investigations on heavy ion collision dynamics [1, 2, 3, 4, 5, 6, 7, 8, 9, 10]. Many studies of the 1-th and 2-nd anisotropic flows, namely the directed flow and elliptic flow, respectively, revealed much interesting physics about the properties and origin of the collective flows. In particular, recent ultra-relativistic Au + Au collision experiments demonstrated the number of constituent-quark (NCQ) scaling from the transverse momentum dependence of the elliptic flow for different mesons and baryons at the Relativistic Heavy Ion Collider (RHIC) in Brookhaven National Laboratory (BNL) [11], it indicates that the partonic degree of the freedom plays a dominant role in formation of the dense matter in the early stage of collisions. Several theoretical models were proposed to interpret the NCQ-scaling of hadrons at RHIC [12, 13, 14, 15, 16]. Of which, a popular interpretation is assuming that mesons and baryons are formed by the coalescence or recombination of the constituent quarks. While at intermediate energy heavy ion collisions, the coalescence mechanism has been also used to explain the formation of light fragments and their spectra of kinetic energy or momentum of light particles some times ago [17, 18, 19, 20, 21]. A few studies investigated the mass dependence of the directed flow [22, 23]. However, systematic theoretical studies on the elliptic flow of different nuclear fragments in intermediate energy domain in terms of the coalescence mechanism is rare.

In this work, we will investigate the flow scaling of hadrons and of nuclear fragments with different microscopic transport theories, namely the partonic transport model in ultra-relativistic energies and nucleonic transport model at intermediate energies, respectively. A common naive coalescence mechanism in quark level or nucleonic

level was applied to analyze the flow. Hadrons, namely baryons and mesons, can be formed by the quark-level coalescence. While, nuclear fragments can be formed by the nucleon-level coalescence. Dependences of the number-of-constituent-quark or number-of-nucleon (NN) of the elliptic flow are surveyed, respectively, and the ratio of v_4 and v_2^2 is studied.

Two examples are given to illustrate the NCQ or NN scaling of the elliptic flow in ultra-relativistic and intermediate energy HIC, respectively. A Multi-Phase Transport (AMPT) model was applied to simulate Au+Au at $\sqrt{s} = 200$ GeV/c for the former case and Isospin-Dependent Molecular Dynamics (IDQMD) was used to simulate $^{86}\text{Kr} + ^{124}\text{Sn}$ at $E_{beam}/A = 25$ MeV/u for the later case.

DEFINITION OF ANISOTROPIC FLOW AND MODEL INTRODUCTION

Definition of anisotropic flow

Anisotropic flow is defined as the different n -th harmonic coefficient v_n of an azimuthal Fourier expansion of the particle invariant distribution [2]

$$\frac{dN}{d\phi} \propto 1 + 2 \sum_{n=1}^{\infty} v_n \cos(n\phi), \quad (1)$$

where ϕ is the azimuthal angle between the transverse momentum of the particle and the reaction plane. Note that in the coordinate system the z -axis along the beam axis, and the impact parameter axis is labelled as x -axis. The first harmonic coefficient v_1 represents the directed flow, $v_1 = \langle \cos\phi \rangle = \langle \frac{p_x}{p_t} \rangle$, where $p_t = \sqrt{p_x^2 + p_y^2}$ is transverse momentum. v_2 represents the elliptic flow which characterizes the eccentricity of the particle distribution in momentum space,

$$v_2 = \langle \cos(2\phi) \rangle = \langle \frac{p_x^2 - p_y^2}{p_t^2} \rangle, \quad (2)$$

and v_4 represents the 4-th momentum anisotropy,

$$v_4 = \left\langle \frac{p_x^4 - 6p_x^2p_y^2 + p_y^4}{p_t^4} \right\rangle. \quad (3)$$

Partonic/hadronic transport model: AMPT model

AMPT (A Multi-Phase Transport) model [24] is a hybrid model which consists of four main processes: the initial condition, partonic interactions, the conversion from partonic matter into hadronic matter and hadronic interactions. The initial condition, which includes the spatial and momentum distributions of minijet partons and soft

string excitation, are obtained from the HIJING model [25]. Excitation of strings melt strings into partons. Scatterings among partons are modelled by Zhang's parton cascade model (ZPC) [26], which at present includes only two-body scattering with cross section obtained from the pQCD with screening mass. In the default version of the AMPT model [27] partons are recombined with their parent strings when they stop interaction, and the resulting strings are converted to hadrons by using a Lund string fragmentation model [28]. In the string melting version of the AMPT model (we briefly call it as "the melting AMPT" model)[29], a simple quark coalescence model is used to combine partons into hadrons. Dynamics of the subsequent hadronic matter is then described by A Relativistic Transport (ART) model [30]. Details of the AMPT model can be found in a recent review [24]. It has been shown that in previous studies [29] the partonic effect can not be neglected and the melting AMPT model is much more appropriate than the default AMPT model when the energy density is much higher than the critical density for the QCD phase transition [24, 29, 16]. In the present work, the partonic interacting cross section in AMPT model with string melting is selected as 10mb.

Nucleonic transport model: QMD Model

The Quantum Molecular Dynamics (QMD) approach is an n-body theory to describe heavy ion reactions from intermediate energy to 2 A GeV. It includes several important parts: the initialization of the target and the projectile nucleons, the propagation of nucleons in the effective potential, the collisions between the nucleons, the Pauli blocking effect and the numerical tests. A general review about QMD model can be found in [31]. The IDQMD model is based on QMD model affiliating the isospin factors, which includes the mean field, two-body nucleon-nucleon (NN) collisions and Pauli blocking [32, 33, 34, 35, 36].

In the QMD model each nucleon is represented by a Gaussian wave packet with a width \sqrt{L} (here $L = 2.16 \text{ fm}^2$) centered around the mean position $\vec{r}_i(t)$ and the mean momentum $\vec{p}_i(t)$,

$$\psi_i(\vec{r}, t) = \frac{1}{(2\pi L)^{3/4}} \exp\left[-\frac{(\vec{r} - \vec{r}_i(t))^2}{4L}\right] \exp\left[-\frac{i\vec{r} \cdot \vec{p}_i(t)}{\hbar}\right]. \quad (4)$$

The nucleons interact via nuclear mean field and nucleon-nucleon collision. The nuclear mean field can be parameterized by

$$U(\rho, \tau_z) = \alpha\left(\frac{\rho}{\rho_0}\right) + \beta\left(\frac{\rho}{\rho_0}\right)^\gamma + \frac{1}{2}(1 - \tau_z)V_c + C_{sym}\frac{(\rho_n - \rho_p)}{\rho_0}\tau_z + U^{Yuk} \quad (5)$$

with ρ_0 the normal nuclear matter density (here, 0.16 fm^{-3} is used). ρ , ρ_n and ρ_p are the total, neutron and proton densities, respectively. τ_z is zth component of the isospin degree of freedom, which equals 1 or -1 for neutrons or protons, respectively. The coefficients α , β and γ are parameters for nuclear equation of state (EOS). C_{sym} is the symmetry energy strength due to the difference of neutron and proton. In the present work, we take $\alpha = -124 \text{ MeV}$, $\beta = 70.5 \text{ MeV}$ and $\gamma = 2.0$ which corresponds to the so-called hard EOS

with an incompressibility of $K = 380$ MeV and $C_{sym} = 32$ MeV [31]. V_c is the Coulomb potential, U^{Yuk} is Yukawa (surface) potential.

The time evolution of the colliding system is given by the generalized variational principal. Since the QMD can naturally describe the fluctuation and correlation, we can study the nuclear clusters in the model [31, 32, 33, 34, 35, 36]. In QMD model, nuclear clusters are usually recognized by a simple coalescence model: i.e. nucleons are considered to be part of a cluster if in the end at least one other nucleon is closer than $r_{min} \leq 3.5$ fm in coordinate space and $p_{min} \leq 300$ MeV/c in momentum space [31]. This mechanism has been extensively applied in transport theory for the cluster formation.

NUMBER-OF-CONSTITUENT-QUARK SCALING OF THE ELLIPTIC FLOW AT RHIC ENERGIES

In non-central Au+Au collisions at RHIC energies, the overlap region is anisotropic (nearly elliptic). Large pressure built up in the collision center results in pressure gradient which is dependent on azimuthal angle, which generates anisotropy in momentum space, namely elliptic flow. Once the spatial anisotropy disappears due to the anisotropic expansion, development of elliptic flow also ceases. This kind of self-quenching process happens quickly, therefore elliptic flow is primarily sensitive to the early stage equation of state (EOS) [37].

Since many particles have been investigated already for demonstrating NCQ scaling of elliptic flow at RHIC. However, the study of strangeness particle, ϕ , is rare. Figure 1 shows both the measurement and the calculation of ϕ -meson elliptic flow v_2 at RHIC [38, 39, 40, 41]. For comparison, v_2 of $K^+ + K^-$ and $p + \bar{p}$ from [42] are plotted together. The most striking thing in the figure is that the ϕ -meson has a non-zero v_2 in the hydrodynamic region ($p_T < 2$ GeV/c) and it has a significant v_2 signal for $p_T > 2$ GeV/c which is comparable to that of the $K^+ + K^-$. Since the formation of ϕ -meson through kaon coalescence at RHIC has been ruled out by previous STAR measurement [43], and the low interaction cross-section of ϕ -meson makes the contribution to flow due to hadronic re-scattering processes very small [24], it may be possible to directly measure the flow of strange quark via the flow of ϕ -meson. Additionally, since the ϕ -meson v_2 values as a function of p_T are similar to those of other particles, this means that the heavier s -quarks flow as much as the lighter u and d quarks. This can happen if there are a significant number of interactions between the quarks before hadronization. It is the signal of partonic collectivity of the system! A prediction [16] from the naive coalescence model which is implemented in A Multi-Phase Transport (AMPT) model with the string melting scenario [44] is also plotted here. The model describes the data quite well at $p_T > 1.5$ GeV/c. This is another hint of coalescence of strange quark as dominant production mechanism for ϕ -meson. Further evidence can be obtained from the Number-of-Constituent-Quark (NCQ) picture in Figure 1.

The RHIC experimental data demonstrated a scaling relationship between 2-nd flow (v_2) and n -th flow (v_n), namely $v_n(p_t) \sim v_2^{n/2}(p_t)$ [45]. It has been shown [46, 47] that such scaling relation follows from a naive quark coalescence model [13] that only allows quarks with equal momentum to form a hadron. Denoting the meson anisotropic

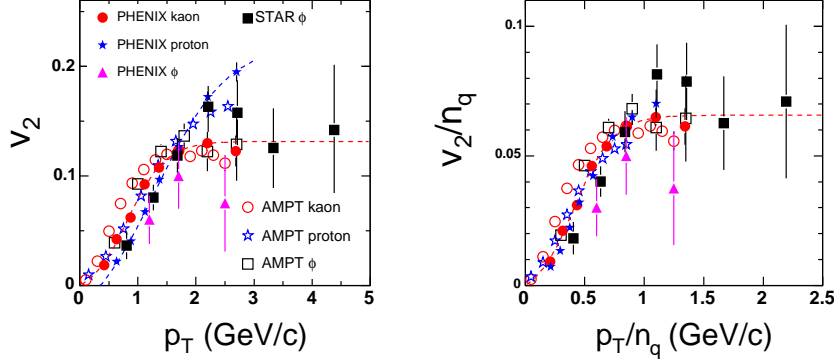


FIGURE 1. Left panel: p_T dependence of v_2 for ϕ -meson which is compared with the cases of $K^+ + K^-$ and $p + \bar{p}$. AMPT calculation are taken from Ref. [16]. Right panel: NCQ scaled v_2 as a function of NCQ scaled transverse momentum. Lines represent NCQ-scaling parameterization.

flows by $v_{n,M}(p_t)$ and baryon anisotropic flows by $v_{n,B}(p_t)$, Kolb et al. found that $v_{4,M}(p_t) = (1/4)v_{2,M}^2(p_t)$ for mesons and $v_{4,B}(p_t) = (1/3)v_{2,B}^2(p_t)$ for baryons if quarks have no higher-order anisotropic flows. Since mesons dominate the yield of charged particles in RHIC experimental data, the smaller scaling factor of 1/4 than the empirical value of about 1 indicates that higher-order quark anisotropic flows cannot be neglected. Including the latter contribution, one can show that

$$\frac{v_{4,M}}{v_{2,M}^2} \approx \frac{1}{4} + \frac{1}{2} \frac{v_{4,q}}{v_{2,q}^2}, \quad \frac{v_{4,B}}{v_{2,B}^2} \approx \frac{1}{3} + \frac{1}{3} \frac{v_{4,q}}{v_{2,q}^2}, \quad (6)$$

where $v_{n,q}$ denotes the quark anisotropic flows. The meson anisotropic flows thus satisfy the scaling relations if the quark anisotropic flows also satisfy such relations. Left panel of Fig. 2 shows the AMPT results for v_2 , v_4 , and v_6 from minimum bias events for Au+Au at $\sqrt{s} = 200$ GeV with parton scattering cross section 10 mb [47]. It is seen that the parton anisotropic flows from the AMPT model indeed satisfy the scaling relation $v_n(p_t) \sim v_2^{n/2}(p_t)$ [47]. However, as shown in the middle panel of Fig. 2, v_4 is experimentally larger than the simulation and the ratio of v_4/v_2^2 is about 1.2 for charged hadrons [45, 48] (see right panel of Fig. 2), which means that the fourth-harmonic flow of quarks v_4^q must be greater than zero. One can go one step further and assume that the observed scaling of the hadronic v_2 actually results from a similar scaling occurring at the partonic level. In this case, if one assumes [46, 47] that the scaling relation for the partons is as follows:

$$v_4^q = (v_2^q)^2, \quad (7)$$

and then hadronic ratio v_4/v_2^2 then equals $1/4 + 1/2 = 3/4$ for mesons and $1/3 + 1/3 = 2/3$ for baryons, respectively. However, since this value is measured to be 1.2 for charged hadrons and pions, so that either the parton scaling relation [Eq. (7)] must have a proportionality constant of about 2, or the simple coalescence model needs improvement.

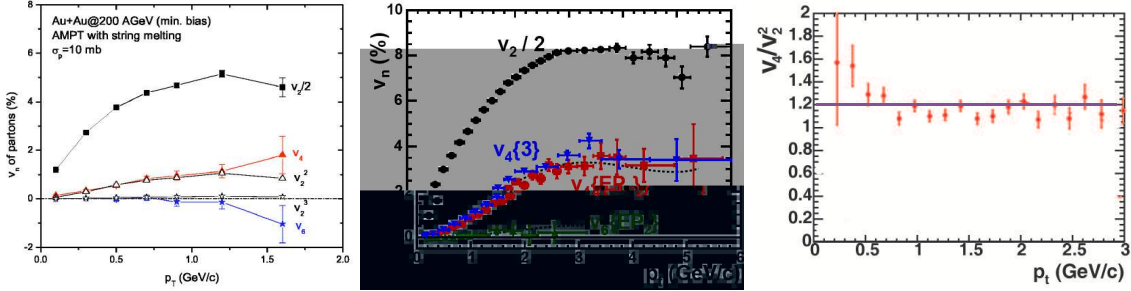


FIGURE 2. (Color online) Left panel (AMPT calculations): Transverse momentum dependence of midrapidity parton anisotropic flows v_2 , v_4 , and v_6 from minimum bias events for Au+Au at $\sqrt{s} = 200$ GeV with parton scattering cross section 10 mb. Also plotted are v_2^2 (open triangles) and v_2^3 (open stars). Figure taken from [47]; Middle panel (STAR data): Minimum bias measurements of anisotropic flow of charged hadrons for different harmonics for Au+Au at $\sqrt{s} = 200$ GeV. The dashed lines show $1.2 v_2^2$ and $1.2 v_2^3$, respectively. Figure taken from [45]; Right panel (STAR data): Ratio of v_4/v_2^2 vs p_T of charged hadrons for Au+Au at $\sqrt{s} = 200$ GeV. The straight line represents the mean of all entries at a value of 1.2 [48].

NUMBER-OF-NUCLEON SCALING OF THE ELLIPTIC FLOW AT INTERMEDIATE ENERGIES

In intermediate energy, we simulated $^{86}\text{Kr} + ^{124}\text{Sn}$ at 25 MeV/nucleon and impact parameter of 7 - 10 fm with IQMD [49]. 50,000 events have been accumulated. The system tends to freeze-out around 120 fm/c. In this work, we extract the following physics results at 200 fm/c. Fig. 3(a) shows transverse momentum dependence of elliptic flows for mid-rapidity light fragments. From the figure, it shows that the elliptic flow is positive and it increases with the increasing p_t . It reflects that the light clusters are preferentially emitted within the reaction plane, and particles with higher transverse momentum tend to be strongly emitted within in-plane, i.e. stronger positive elliptic flow. In comparison to the elliptic flow at RHIC energies, the apparent behavior of elliptic flow versus p_t looks similar, but the mechanism is obviously different. In intermediate energy domain, collective rotation is one of the main mechanisms to induce the positive elliptic flow [50, 51, 52, 53, 54, 55]. In this case, the elliptic flow is mainly driven by the attractive mean field. However, the strong pressure which is built in early initial geometrical almond-type anisotropy due to the overlap zone between both colliding nuclei in coordinate space will rapidly transforms into the azimuthal anisotropy in momentum space at RHIC energies [11]. In other words, the elliptic flow is mainly driven by the stronger outward pressure. Fig. 3(b) displays the elliptic flow per nucleon as a function of transverse momentum per nucleon, and it looks that there exists the number of nucleon scaling when $p_t/A < 0.25$ GeV/c. This behavior is apparently similar to the number of constituent quarks scaling of elliptic flow versus transverse momentum per constituent quark (p_t/n) for mesons and baryons which was observed at RHIC [11] and shown in Fig. 3(b).

Recognizing the v_4/v_2^2 behaviors at RHIC energies, we would like to know what the higher order momentum anisotropy in the intermediate energy is. So far, there is

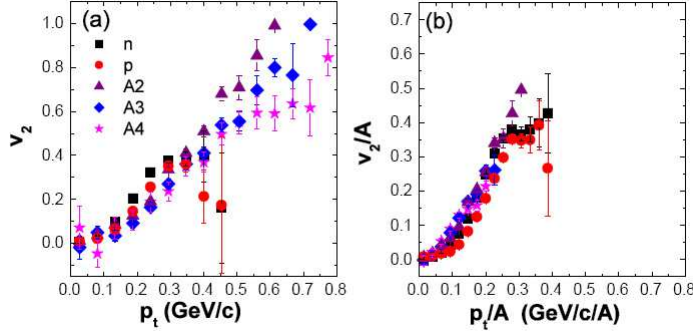


FIGURE 3. (a) Elliptic flow as a function of transverse momentum (p_t). Squares represent for neutrons, circles for protons, triangles for fragments of $A = 2$, diamonds for $A = 3$ and stars for $A = 4$; (b) Elliptic flow per nucleon as a function of transverse momentum per nucleon. The symbols are the same as (a).

neither experimental data nor theoretical investigation for the higher order flow, such as v_4 , in this energy domain. In the present work, we explore the behavior of v_4 in the model calculation. Fig. 4 shows the feature of v_4 . Similar to the relationship of v_2/A versus p_t/A , we plot v_4/A as a function of p_t/A . The divergence of the different curves between different particles in Fig. 4(a) indicates no simple scaling of nucleon number for 4-th momentum anisotropy. However, if we plot v_4/A^2 versus $(p_t/A)^2$, it looks that the points of different particles nearly merge together and it means a certain of scaling holds between two variables. Due to a nearly constant value of v_4/v_2^2 in the studied p_t range (see Fig. 4(c)) together with the number-of-nucleon scaling behavior of v_2/A vs p_t/A , v_4/A^2 should scale with $(p_t/A)^2$, as shown in Fig. 4(b). If we assume the scaling laws of mesons (Eq. 6) are also valid for $A = 2$ and 3 nuclear clusters, respectively, then v_4/v_2^2 for $A = 2$ and 3 clusters indeed give the same value of $1/2$ as nucleons, as shown in Fig. 4(c). Coincidentally the predicted value of the ratio of v_4/v_2^2 for hadrons is also $1/2$ if the matter produced in ultra-relativistic heavy ion collisions reaches to thermal equilibrium and its subsequent evolution follows the laws of ideal fluid dynamics [56]. It is interesting to note the same ratio was predicted in two different models at very different energies, which is of course worth to be further investigated in near future. Overall speaking, we learn that v_4/v_2^2 is approximately $1/2$ in nucleonic level coalescence mechanism, which is different from $3/4$ for mesons or $2/3$ for baryons in partonic level coalescence mechanism.

SUMMARY

In summary, we applied AMPT and IDQMD model to investigate the behavior of anisotropic flows, namely v_2 and v_4 , versus transverse momentum for hadrons in Au+Au at $\sqrt{s_{nn}} = 200$ GeV/c as well as light nuclear fragments for 25 MeV/nucleon $^{86}\text{Kr} + ^{124}\text{Sn}$ collisions at 7-10 fm of impact parameters. Both v_2 and v_4 generally show positive values and increase with p_t in two very different energies. By the number scaling of constituent-quarks or nucleons, the curves of elliptic flow for different hadrons or nuclear fragments approximately collapse on the similar curve, respectively, which means that there exists

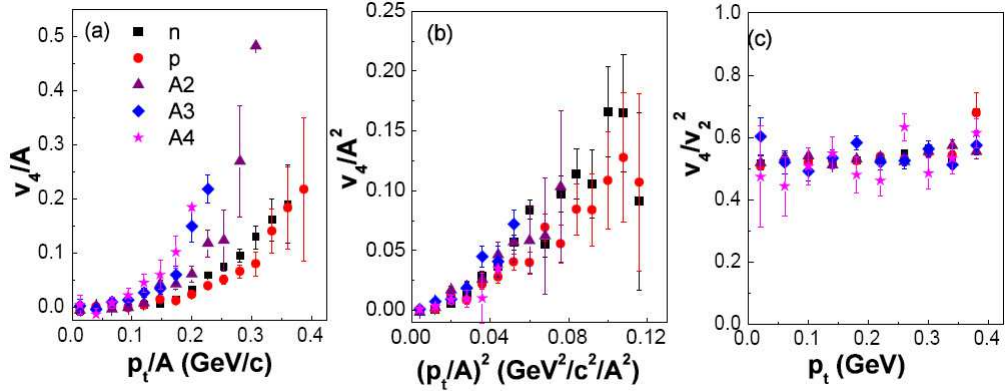


FIGURE 4. (a) v_4/A as a function of p_t/A for different particles, namely, neutrons (squares), protons (circles), fragments of $A = 2$ (triangles), $A = 3$ (diamonds) and $A = 4$ (stars). (b) v_4/A^2 as a function of $(p_t/A)^2$. (c) the ratios of v_4/v_2^2 for different particles vs p_t .

an elliptic flow scaling on the constituent quark number or nucleon number. NCQ scaling stems from the partonic coalescence and NN scaling originates from nucleonic coalescence. For 4-th momentum anisotropy v_4 , it seems to be scaled by v_2^2 , and v_4/v_2^2 is different for hadrons and nuclear fragments. AMPT predicts a smaller value of v_4/v_2^2 than the data ~ 1.2 and the value of nuclear fragments ~ 0.5 . The former indicates that either the parton scaling relation [Eq. (7)] must have a proportionality constant of about 2, or the simple quark coalescence model needs improvement. For the later, the data is unable to be available yet. Therefore it will be of very interesting if one can measure this ratio in intermediate energy HIC.

ACKNOWLEDGEMENTS

Author appreciate my collaborators and friends, especially to X. Z. Cai, J. H. Chen, G. L. Ma, T. Z. Yan, H. Z. Huang and W. Q. Shen. This work was supported in part by the Shanghai Development Foundation for Science and Technology under Grant Numbers 05XD14021 and 06JC14082, the National Natural Science Foundation of China under Grant No 10535010, 10328259 and 10135030.

REFERENCES

1. J. Ollitrault, Phys. Rev. D 46 (1992) 229.
2. S. Voloshin, Y. Zhang, Z. Phys. C 70 (1996) 665.
3. H. Sorge, Phys. Lett. B 402 (1997) 251; Phys. Rev. Lett. 78 (1997) 2309 ; 82 (1999) 2048.
4. P. Danielewicz, R. A. Lacey, P. B. Gossiaux et al., Phys. Rev. Lett. 81 (1998) 2438.
5. B. Zhang, M. Gyulassy, and C. M. Ko, Phys. Lett. B 455(1999) 45.
6. D. Teaney and E. V. Shuryak, Phys. Rev. Lett. 83 (1999) 4951.
7. P. F. Kolb, J. Sollfrank, and U. Heinz, Phys. Rev. C 62 (2000) 054909.
8. Y. Zheng, C. M. Ko, B. A. Li, and B. Zhang, Phys. Rev. Lett. 83 (1999) 2534.
9. D. Perslam and C. Gale, Phys. Rev. C 65 (2002) 064611.

10. J. Lukasik et al. (INDRA-ALDAIN Collaboration), *Phys. Lett. B* 608 (2004) 223.
11. J. Adams et al., *Phys. Rev. Lett.* 92 (2004) 052302; *Phys. Rev. C* 72 (2005) 014904; *Phys. Rev. Lett.* 95 (2005) 122301;
12. Zi-Wei Lin and C. M. Ko, *Phys. Rev. Lett.* 89 (2002) 202302; V. Greco, C. M. Ko, and P. Lévai, *Phys. Rev. C* 68 (2003) 034904 .
13. D. Molnár and S. A. Voloshin, *Phys. Rev. Lett.* 91 (2003) 092301.
14. R. J. Fries, B. Müller, C. Nonaka, and S. A. Bass, *Phys. Rev. Lett.* 90 (2003) 202303; *Phys. Rev. C* 68 (2003) 044902.
15. R. C. Hwa and C. B. Yang, *Phys. Rev. C* 66 (2002) 025205; *Phys. Rev. C* 70 (2004) 024904.
16. J. H. Chen, Y. G. Ma, G. L. Ma et al., Proceeding for the "Workshop on Quark-Gluon-Plasma Thermalization", Vienna, Austria; *Eur. Phys. J. A*29 (2006) 11.
17. T. C. Awes, G. Poggi, C. K. Gelbke et al., *Phys. Rev. C* 24 (1981) 89.
18. A. Z. Mekjian, *Phys. Rev. C* 17 (1978) 1051; *Phys. Rev. Lett.* 38 (1977) 640; *Phys. Lett.* 89B (1980) 177 .
19. H. Sato and K. Yazaki, *Phys. Lett.* 98B (1981) 153.
20. W. J. Llope, S. E. Pratt, N. Frazier et al., *Phys. Rev. C* 52 (1995) 002004.
21. K. Hagel, R. Wada, J. Cibor et al., *Phys. Rev. C* 62 (2000) 034607.
22. M. J. Huang, R. C. Lemmon, F. Daffin, et al., *Phys. Rev. Lett.* 77 (1996) 3739 .
23. G. J. Kunde, W. C. Hsi, W. D. Kunze et al., *Phys. Rev. Lett.* 74 (1995) 38.
24. Z. W. Lin, C. M. Ko, B. A. Li, B. Zhang, S. Pal, *Phys. Rev. C* 72 (2005) 064901.
25. X.-N. Wang and M. Gyulassy, *Phys. Rev. D* 44 (1991) 3501; M. Gyulassy and X.-N. Wang, *Comput. Phys. Commun.* 83 (1994) 307.
26. B. Zhang, *Comput. Phys. Commun.* 109 (1998) 193.
27. B. Zhang, C. M. Ko et al., *Phys. Rev. C* 61 (2000) 067901 .
28. B. Andersson, G. Gustafson et al., *Phys. Rep.* 97 (1983) 31.
29. Z. W. Lin, C. M. Ko, *Phys. Rev. C* 65 (2002) 034904; Z. W. Lin, C. M. Ko et al., *Phys. Rev. Lett.* 89 (2002) 152301.
30. B. A. Li and C. M. Ko, *Phys. Rev. C* 52 (1995) 2037.
31. J. Aichelin, *Phys. Rep.* 202 (1991) 233.
32. Y. G. Ma and W.Q. Shen, *Phys. Rev. C* 51 (1995) 710.
33. J.Y. Liu, Y.F. Yang, W. Zuo et al., *Phys. Rev. C* 63 (2001) 54612.
34. Y. B. Wei, Y. G. Ma, W. Q. Shen et al., *Phys. Lett. B* 586 (2004) 225; *J. Phys. G* 30 (2004) 2019.
35. Y. G. Ma, H. Y. Zhang and W. Q. Shen, *Prog. Phys. (in Chinese)* 22 (2002) 99.
36. Y. G. Ma, Y. B. Wei, W. Q. Shen et al., *Phys. Rev. C* 73 (2006) 014604.
37. P. Huovinen 2003 *arxiv:nucl-th/0305064*; P. Kolb and U. Heinz 2003 *arxiv:nucl-th/0305084*; E. V. Shuryak 2004 *Prog. Part. Nucl. Phys.* 53 (2004) 274.
38. X. Z. Cai (for the STAR Collaboration), *Nucl. Phys. A* 774 (2006) 485.
39. J. H. Chen and S-L. Blyth et al. (for the STAR Collaboration), in preparation.
40. D. Pal (for the PHENIX Collaboration) *Nucl. Phys. A* 774 (2006) 489.
41. Y. G. Ma, *J. Phys. G* 32 (2006) S373.
42. S. S. Adler et al. (for the PHENIX Collaboration), *Phys. Rev. Lett.* 91 (2003) 182301.
43. J. Adams et al (for the STAR Collaboration), *Phys. Lett. B* 612 (2006) 181.
44. Z. W. Lin et al., *Phys. Rev. C* 72 (2005) 064901 .
45. J. Adams et al. (for the STAR Collaboration), *Phys. Rev. Lett.* 92 (2004) 062301.
46. P. F. Kolb, L. W. Chen, V. Greco, C. M. Ko, *Phys. Rev. C* 69 (2004) 051901.
47. L. W. Chen, C. M. Ko, Zi-Wei Lin, *Phys. Rev. C* 69 (2004) 031901(R).
48. J. Adams et al. (for the STAR Collaboration), *Phys. Rev. C* 72 (2005) 014904.
49. T. Z. Yan, Y. G. Ma, X. Z. Cai et al., *Phys. Lett. B* 638 (2006) 50.
50. For a review, see W. Reisdorf and H. G. Ritter, *Annu. Rev. Nucl. Part. Sci.* 47 (1997) 663.
51. J. P. Sullivan and J. Péter, *Nucl. Phys. A* 540 (1992) 275.
52. W. Q. Shen, J. Péter, G. Bizard et al., *Nucl. Phys. A* 551 (1993) 333.
53. Y. G. Ma et al., *Phys. Rev. C* 48 (1993) R1492; *Z. Phys. A* 344 (1993) 469; *Phys. Rev. C* 51 (1995) 1029; *Phys. Rev. C* 51 (1995) 3256.
54. R. Lacey, A. Elmaani, J. Lauret et al., *Phys. Rev. Lett.* 70 (1993) 1224.
55. Z. Y. He, J.C. Angelique, A. Auger et al., *Nucl. Phys. A* 598 (1996) 248.
56. N. Borghini and J-Y. Ollitrault, *nucl-th/0506045*.